Effects of booms of sounding rockets in flowing plasmas

J. J. P. Paulsson,[1] Y. Miyake,[2] W. J. Miloch,[1] and H. Usui[2]

[1)] *Department of Physics, University of Oslo, Oslo, Norway*[a)]

[2)] *Graduate School of System Informatics, Kobe University, Kobe, Japan*

(Dated: 8 August 2018)

The effect of booms of a sounding rocket on the spacecraft charging in flowing ionospheric plasmas and on the local plasma conditions is studied with numerical and analytical models. The simulations are carried with a first principle self-consistent Particle-In-Cell numerical code. It is shown that the booms can affect the charging of the payload and disturb the local plasma to a high degree. The boom-to-plasma potential, which should differ position by position due to the convective electric field, can lead to significantly different currents to the booms on either of the rocket, in particular the electron currents. The analytical models for the collected currents considered in this study show good agreement with the simulations. The potential difference between the plasma and the surface of the rocket can focus the ions to create regions of enhanced ion density downstream of the rocket, and can cause the wake downstream to have an asymmetric profile. It is shown that the ion focusing can be asymmetric between the booms due to the potential gradient. These effects can have implications for the instrument placements and data analysis.

PACS numbers: Valid PACS appear here

Keywords: Suggested keywords

[a)]Electronic mail: j.j.p.paulsson@fys.uio.no

I. INTRODUCTION

Charging of spacecraft in space is an important issue not only for protection of payload circuits, but also for performing in situ measurements with instruments onboard spacecraft[1,2]. Examples of such instruments are Langmuir probes, which for their operation often need to attain a specific electric potential bias with respect to plasma[3,4]. Since the payload provides the potential bias, it will be seen as ground by the probe. If the payload and spacecraft are electrically conducting, they will attain a floating equipotential[2]. Thus, for proper data analysis and operation of payload instruments, it is essential to have a good knowledge on the spacecraft potential under plasma conditions relevant for particular space missions.

In general, there are many different space plasma environments relevant for spacecraft missions, ranging from the ionosphere (relevant for sounding rockets)[5–8], where the Debye length is generally shorter than the typical length scale of the payload, to interplanetary space[9,10], where the Debye length can be much larger than the spacecraft. Using sounding rockets to study ionospheric plasmas with in situ measurements poses some unique problems, but it also benefits by allowing for launching a rocket in a relatively short time-span to investigate short-lived or fast traveling structures[5,8]. In order to be able to correctly analyze data collected by the sounding rocket payload instruments, one needs to understand the charging of the payload, and how payload interacts with the surrounding plasma.

Charged ionospheric rocket will affect plasma in its vicinity mainly through electrostatic sheath or through the development of wake[1,11,12]. The extent of electrostatic sheath is usually of an order of the Debye length, while the extent of wake, which forms downstream of a rocket moving with respect to plasma, depends on the plasma flow speed[13–15]. In an effort to avoid these effects, booms might be attached to the payload. Mounting instruments on such booms will decrease a disturbance in plasma due to the rocket. This is certainly true regarding the electrostatic sheath, where already a short boom would be able to reach outside the perturbed region in the ionosphere. The wake on the other hand may extend very far downstream. In fact, Al'pert, Gurevich, and Pitaevski[11] indicate that the wake may be divided in two regions: the first region, close to the body, which is dominated by the potential of the rocket body; and the second region, far away from the rocket, which is dominated by shadowing of ion trajectories in phase-space. Depending on the thermal velocity of ions, the flow speed of plasma, and the rocket geometry, the extent of the first

region may be of the order of hundreds of Debye lengths[16]. Hence, attaching stable booms that are able to extend far enough from the rocket, such that instruments can be allowed to experience mostly undisturbed plasma, is a non-trivial task. Thus, a good knowledge how the rocket-plasma interaction is required to interpret data from such instruments.

Furthermore, due to complex geometry of a rocket with a boom system attached, its complete interaction with the surrounding plasma is unpredictable with analytical approaches. This is valid not only for the plasma in its vicinity, but also for charging of the payload. The main body of the payload is often much larger than the Debye length and shaped like a cylinder, whereas the radius of the booms can often be comparable with the Debye length. This means that the plasma currents collected by the main body and booms may need to be addressed by different approaches.

The convective electric field in the ionosphere, as experienced by the rocket, i.e., in a reference frame fixed at the rocket body, will create a potential difference on tips of the booms if they are aligned with vector components of the electric field. As a result, the potential difference between the plasma and the floating potential of the boom on either side of it will be different and related to the electric field strength and the boom length. Not only will this affect charging of the rocket, but it can lead to asymmetries in the density distribution at different sides of the spacecraft.

In this work, we address the problem of interaction of plasma with a cylindrically shaped rocket with booms in a self-consistent way, by employing numerical simulations. The simulations are carried out with the Particle-In-Cell (PIC) computer code. We consider different plasma flow velocities and compare results to analytical theories. We demonstrate that the presence of booms has non-trivial effects on the charging of the rocket and the plasma distribution in the vicinity of the rocket body.

II. METHOD

To study the role of booms for rocket-charging and rocket-plasma interaction, we employ a PIC numerical code, EMSES[9]. The details on the EMSES code are given in previous works[9], and here we provide only the main idea behind the algorithm and parameters used for the study. In the PIC method, the plasma particles (i.e., electrons and ions) interact with each other via computational grid that is used to calculate force fields. This reduces

Parameter	Symbol	Value
Plasma density (m^{-3})	n_0	$2 \cdot 10^{11}$
Electron temperature (K)	T_e	3000
Ion temperature (K)	T_i	2000
Mach number	M	$0.5 - 8.0$
Magnetic field (μT)	B	50
Ion-to-electron mass ratio	m_i/m_e	500
Debye length (cm)	λ_D	0.845
Box size (cm)	L	32.95

TABLE I. List of parameters used in the simulation

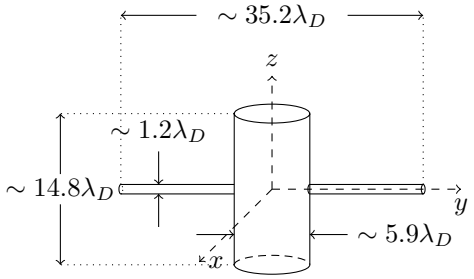

FIG. 1. Schematic of the simulated rocket and booms with their sizes and a coordinate system.

the computational cost and makes it feasible to simulate large plasma systems[17]. The main computational cycle consists of 1) weighting numerical particles to the nearest grid points, 2) solving the field equations and finding forces on the grid, 3) projecting forces from grid points to particles, 4) advancing particle trajectories according to equations of motion. Thus, in the PIC method, we can study a self-consistent evolution of the system based on first principles.

A rocket with booms is placed on a Cartesian grid and forms internal boundary conditions for the plasma particle trajectories, see FIG 1. It is placed inside a simulation box of $39\lambda_D$ in each direction, where $\lambda_D = \sqrt{\epsilon_0 k_B T_e / n e^2}$ is the electron Debye length, where ϵ_0 k_B, T_e, n_0, e are respectively the electron permittivity of vacuum, Boltzmann constant, electron temperature, plasma density and electron charge. The size of the rocket and the booms are

respectively $14.8\lambda_D$ and $35.2\lambda_D$, thus ensuring that the main rocket body is far from the boundaries, and that there are no boundary effects affecting the boom charging. Charged plasma particles hitting the surface of the rocket contribute to its surface charge. For computational reasons it is not possible to simulate the actual size of typical ionospheric sounding rocket with the booms, which often have a tip-to-tip length more than 1 meter. However, we use a scaled system which can be used as a model case, where the ratios between the Debye length and rocket and boom sizes are maintained. The rocket surface is equipotential, which is achieved in the numerical simulation with the capacitance matrix method[9,17]. The simulation domain is open for plasma particles and can account for the plasma flow. While EMSES is an electromagnetic code, in the present study we work in the electrostatic approximation with external static magnetic field.

The simulated plasma parameters are relevant for ionospheric plasma conditions, and are summarized in TABLE I. The background plasma density is $n_0 = 2 \cdot 10^{11}\mathrm{m}^{-3}$, the electron and ion temperatures are respectively $T_e = 3000$ K and $T_i = 2000$ K, and the ion to electron mass ratio $m_i/m_e = 500$, which is large enough to separate the dynamics of electrons and ions, but still allows for a reasonable time of simulations. The background magnetic field is $B = 50\mu$T. We consider the plasma flow velocities v_d in the range of $M \in (0.5, 8)$ with increments for 0.5 for each simulation, where M is the Mach number $M = v_d/C_s$, and $C_s = \sqrt{k_B T_e/m_i}$ is the sound speed. The flow is perpendicular to the rocket axis and booms, and the geometry and dimensions of the rocket are shown in FIG 1, together with the coordinate system. The magnetic field vector is always pointing in the positive z-direction, the plasma flow velocity $\mathbf{v_d}$ is directed in the positive x-direction, following the electric field, corresponding to the $\mathbf{E} \times \mathbf{B}$-drift in the positive y-direction. The main body of the rocket is aligned with the z-axis, and the booms with the y-axis.

III. RESULTS

We perform a series of simulations to study the effect of the boom on the rocket-plasma interaction. FIG. 2 shows simulation results for the ion density for four different Mach numbers. The plasma flow is in the positive x-direction. Notice the ion focusing effects at the end points of the booms, which can be attributed to electrostatic bending of ion trajectories[18]. In FIG. 2 a) there is an even focusing around Boom 1 and Boom 2, but as the

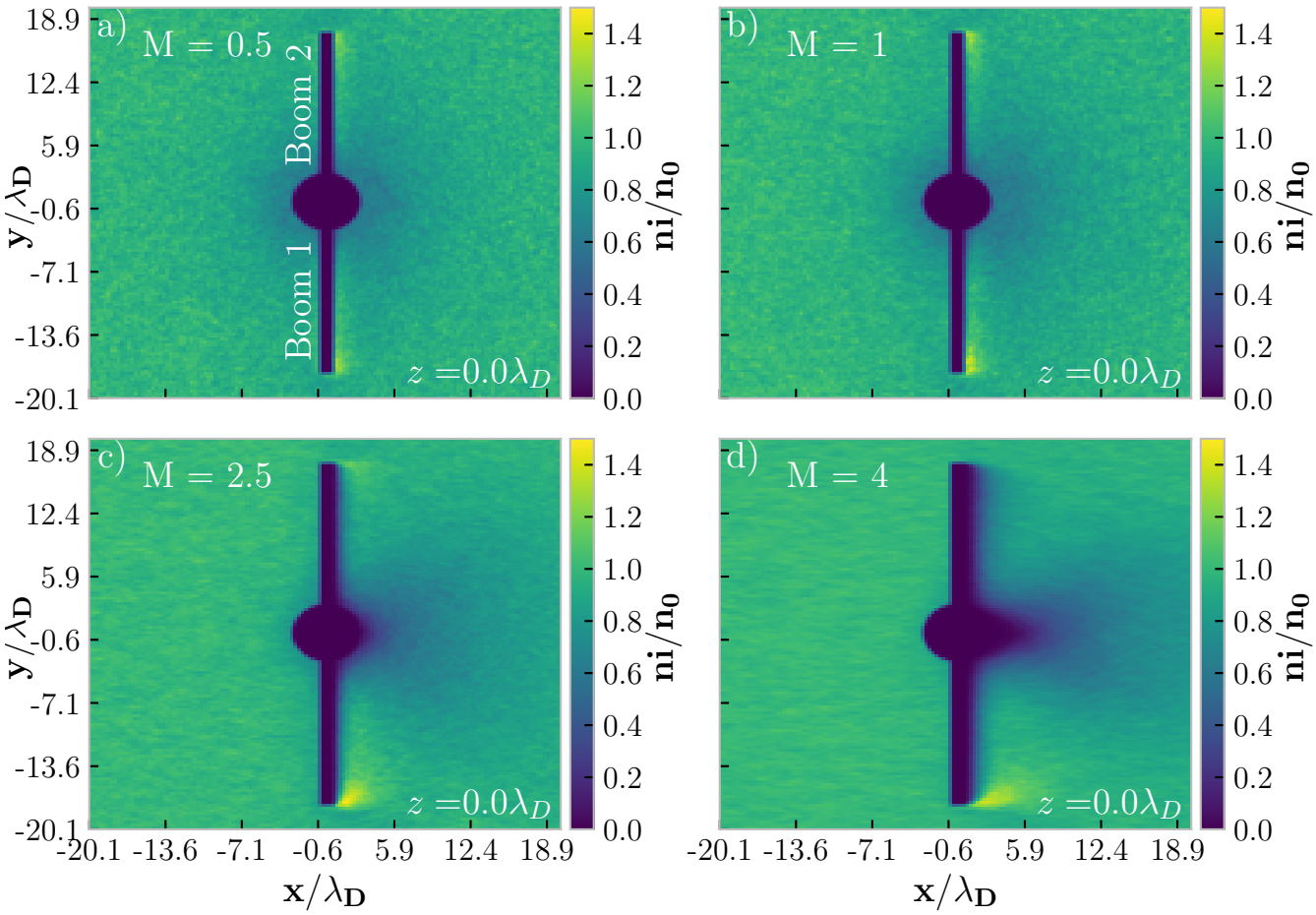

FIG. 2. Normalized distribution of the ion distribution in the x-y plane, at $z = 0$ for different Mach numbers M. a) M=0.5, b) M=1.0, c) M=2.0, d) M=4.0. The plasma flow is in the positive x-direction.

drift velocity increases, the focusing behind Boom 2 decreases, while behind Boom 1 it gets more pronounced. This can be attributed to the convective electric field: When increasing the Mach number while keeping the magnetic field constant, the electric field increases according to $\mathbf{E} = -\mathbf{v_d} \times \mathbf{B} = v_d B \hat{\mathbf{y}}$ and, hence the potential drop between the plasma and the rocket gets larger for Boom 1 than for Boom 2. The potential drop difference between the booms and plasma can be seen in FIG. 3, which gives a cut through the potential along the booms in the y-direction.

The current collected by a conductive body depends on the difference between the electric potential of the object and plasma[3,4]. Therefore, along the length of the booms, each unit section will collect a different current due to the potential gradient from the convective

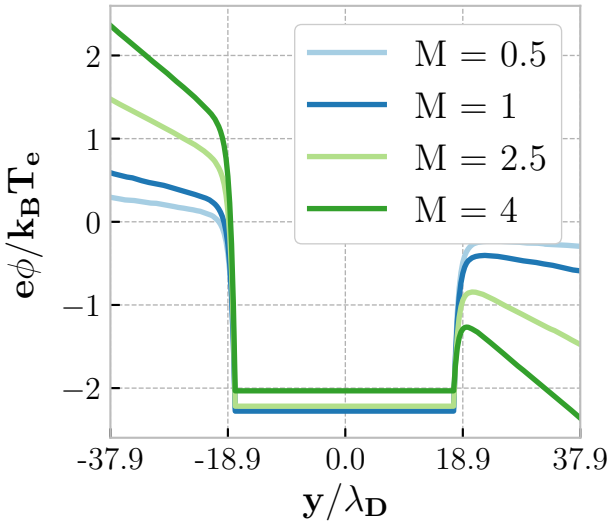

FIG. 3. Potential profile along y for $z = x = 0$. The potential difference between the body (the flat region around y = 0) and the plasma potential is different between the ends of the booms.

electric field. Assuming that the potential difference is $V_b - V_p < 0$, where V_b is the potential of the body and V_p is the plasma potential, for all parts of the boom, the electron current to a cylindrical part of the boom at position y will be:

$$dI_e = 2\pi r dy I_{0e} \exp \frac{e\left(V_b - V_p(y)\right)}{k_B T_e}, \tag{1}$$

where r is the radius of the boom, dy is the length of the cylindrical section of the boom, $I_{0e} = en_e\sqrt{k_B T_e/2\pi m_e}$ is the electron random thermal current, V_b is the potential of the boom, $V_p(y)$ is the plasma potential at position y. Assuming that the convective electric field is the dominant factor determining the plasma potential, we can write:

$$V_p(y) = -v_d B y. \tag{2}$$

Then letting dy go to zero and summing over all the cylindrical sections, i.e., sections from one boom edge y_0 to the other y_1, we obtain the total electron current to the boom:

$$\begin{aligned} I_e =& 2\pi r I_{0e} \exp \frac{eV_b}{k_B T_e} \int_{y_0}^{y_1} \exp \frac{ev_d B y}{k_B T_e} dy \\ =& 2\pi r I_{0e} \frac{k_B T_e}{ev_d B} \exp\left(\frac{eV_b}{k_B T_e}\right)\left(\exp\left(\frac{e}{k_B T_e} v_d B y_1\right)\right. \\ & \left. - \exp\left(\frac{e}{k_B T_e} v_d B y_0\right)\right). \end{aligned} \tag{3}$$

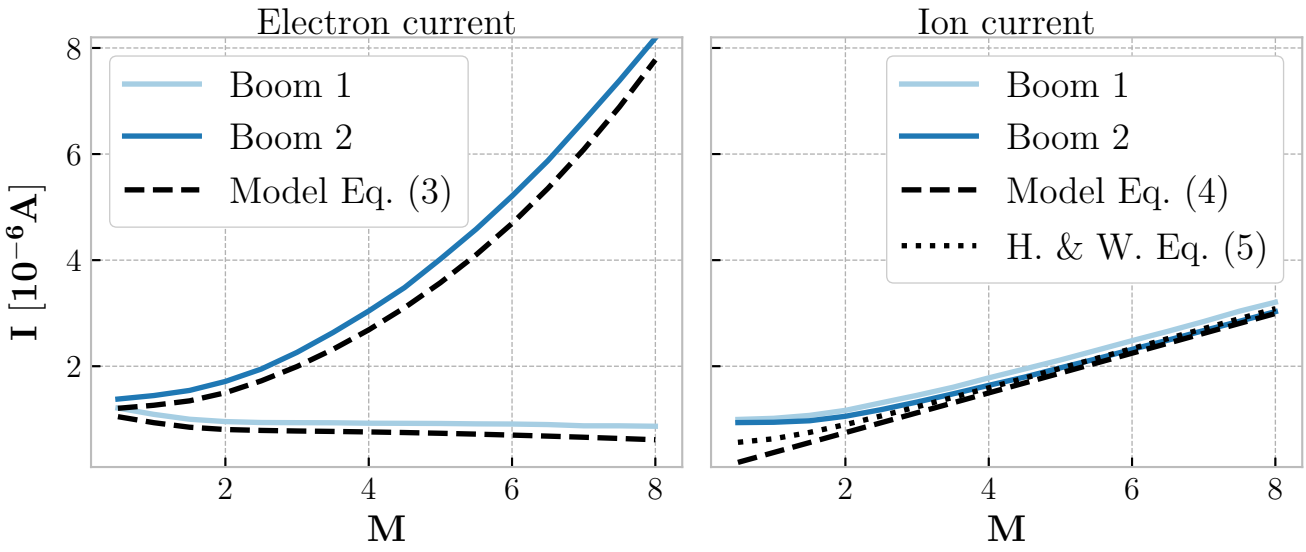

FIG. 4. Electron (left panel) and ion (right panel) currents to the booms versus the Mach number. Left panel; the electron currents from the simulations to the two booms (solid lines) and from the model given by Eq. (3) (dashed lines). Right panel; the ion currents from the simulations to the two booms (solid lines) and from the ion ram current model (dashed line) Eq. (4), as well as Hoegy and Wharton's model (dotted line) Eq. (5).

We can see that the electron current is a non-linear function of the ratio between the drift velocity and the electron temperature; $I_e \sim T_e/v_d \exp(v_d/T_e)$. In the left panel of FIG. 4 we have compared the electron currents to the boom as measured in the simulation with Eq. (3). The simulation and the analytical approximation show good agreement, however there is a slight offset.

The collection of ions by a finite-sized objects is often more involved[19]. However, as the plasma flow velocity increases, one can expect that the cold ion approximation can provide an estimate of the ion current to a higher degree of accuracy. Assuming ions with no thermal motion, the flux to the booms can be expressed by:

$$I_i = 2rLen_i v_d, \tag{4}$$

where L is the boom length. We will refer to this current as the *ram current*.

Hoegy and Wharton[20] derived an expression for an approximate ion current to a cylinder

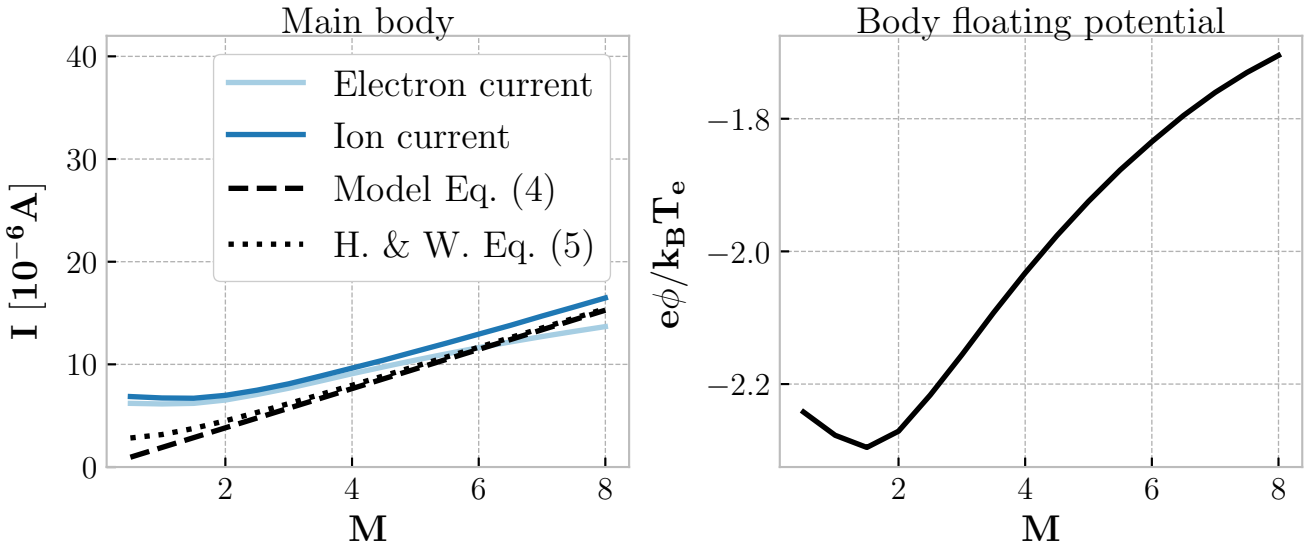

FIG. 5. Electron and ion currents to the main body (left panel) and the body floating potential (right panel) versus the Mach number. Left panel; the electron (solid light blue line) and ion (solid dark blue line) currents from the simulation and the ion ram current model (dashed line) Eq. (4), as well as Hoegy and Wharton's model (dotted line) Eq. (5).

that includes ion thermal effects:

$$I_i = 2\pi r L I_{0i} \frac{2}{\sqrt{\pi}} \left(|V_b - V_p| + S_d^2 + \frac{|V_b - V_p| + S_d^2/2}{|V_b - V_p| + S_d^2} \right)^{1/2}, \tag{5}$$

where $I_{0i} = en_i\sqrt{k_B T_i/2\pi m_i}$, and $S_d = v_d/v_{thi}$ where $v_{thi} = \sqrt{2k_B T_i/m_i}$.

We compare the two approximations with the numerical results in FIG. 4. The right panel of FIG. 4 shows the ion current collected by the two booms, as well as the ion ram current of Eq. (4) and Hoegy and Wharton's ion current calculated with Eq. (5). For low M the ion current differs from the ram current approximation significantly, while Hoegy and Wharton's ion current is consistently closer to the numerical results. As M increases, both analytical results get closer to the simulation results. Note that there is also, albeit small, an increasing difference between the ion currents to the two booms with increasing M.

The currents to the main body are shown in the left panel of FIG. 5 together with the ion currents given by Eq. (4) and Eq. (5). One can see that both the ion and electron currents become closer to the analytical results with increasing M. Note that there is a slight imbalance between the ion and the electron currents to the main body, which increases with

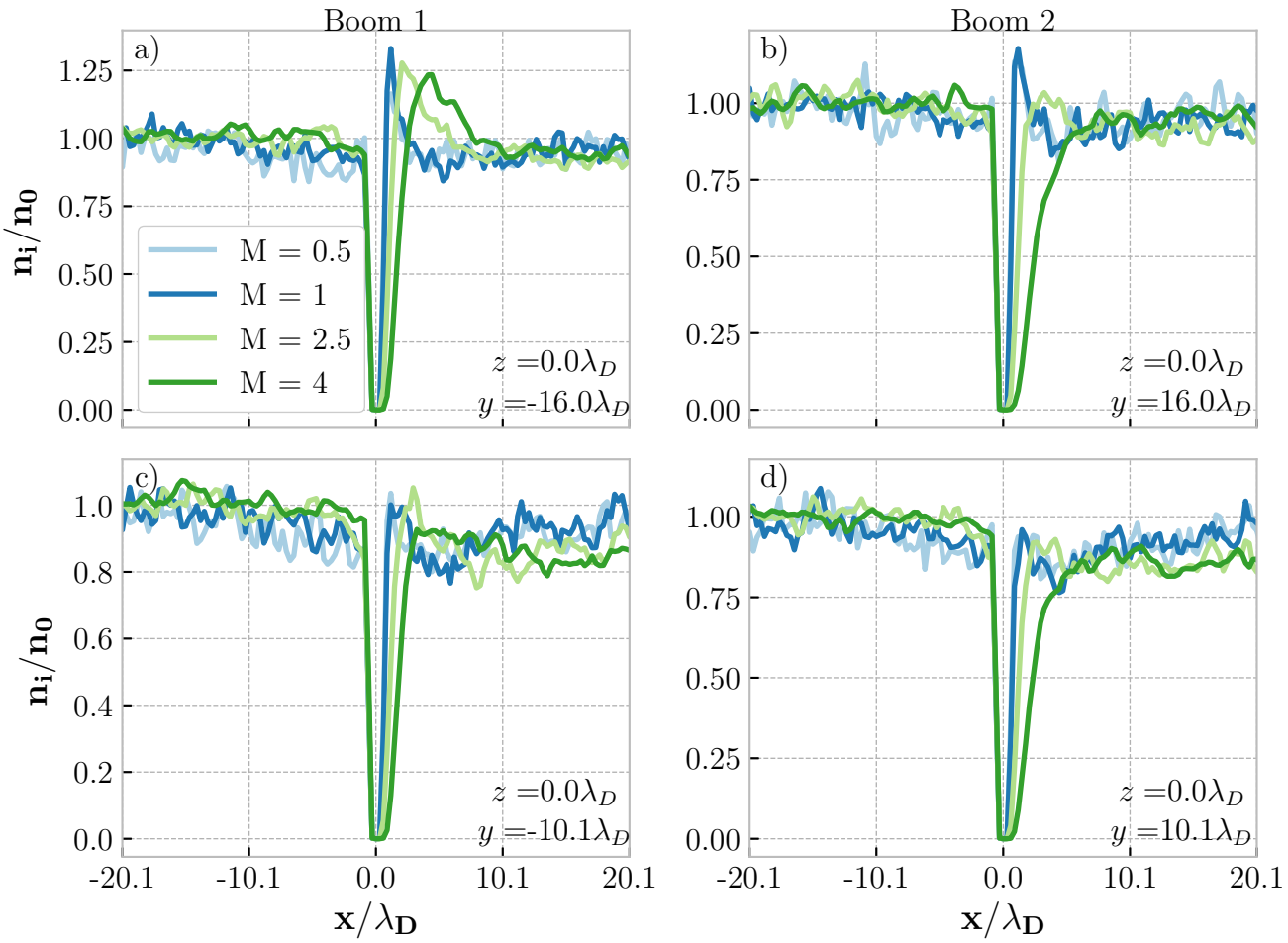

FIG. 6. Profiles of the normalized ion density n_i/n_0 along the x-axis for a fixed y and z across the two booms at different distances from the origin and Mach numbers. See FIG 2 for coordinates for the booms.

increasing M and at $M = 8$ the difference between the ion and the electron current is significant.

The floating potential of the body is shown in the right panel of FIG. 5. The potential starts to dip towards more negative when the flow transitions from subsonic to supersonic speeds, and at around $M = 1.5$ it starts to increase. Note that the increasement of the body potential after the turning point is not linear, even thought the the ion current remains linear as can be seen in the right panel of FIG. 4.

As can be seen in FIG. 2 the plasma around the rocket is disturbed. All parts of the rocket disturb the plasma, but the booms and main body have different effects. Long and thin booms tend to focus ions, and this effect becomes more asymmetric with increasing

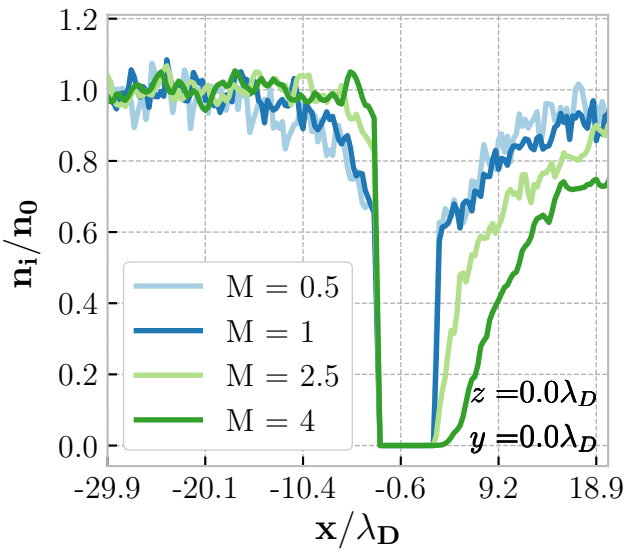

FIG. 7. Profiles of the normalized ion density n_i/n_0 along the x-axis at a fixed $y = 0$ and $z = 0$ across the center of the main body for different Mach numbers.

Mach number. In FIG. 2 panel a) we see a weak focusing downstream of the booms with small asymmetry, but in panel d) there is a significant difference in the ion distribution behind the two booms. In FIG. 6 the ion density profiles across the booms at two different distances from the origin are shown. In FIG. 6 panel a) we see that the maximum ion focus is at $M = 1$ at the tip of Boom 1, but as M increases the maximum in the ion density decreases and the enhanced ion density region extends to larger distances downstream of the boom. Note also that no ion depletion is observed. In panel c), which is at a part of Boom 1 that is closer to the main body, the ion focusing is much less pronounced, and is in fact not present at all for $M = 4$. We can also see that a depletion in plasma density is formed behind this part of the boom. For Boom 2, at the tip, in panel b), the significant focusing is present only for $M = 1$, and almost no wake is formed for all cases, except for $M = 4$. In panel d), for a part of Boom 2 that is closer to the main body, there is little enhancement in the ion density, but the ion depletions get more pronounced.

The corresponding profiles for the main body are shown in FIG. 7. The wakes extend further, up to several Debye lengths, downstream of the main body with increasing M. Upstream of the main body the sheath extends farther for lower M.

Finally, the potential profile downstream of the rocket at increasing distances from the surface of the main body is shown in FIG. 8. Note that the scale of the vertical axis

changes in each of the panels. In panel a) one can see the asymmetry in potential which can be attributed the ion distribution behind the booms. For $M = 4$ the potential reaches a positive value at the left hand side of the wake at this distance. For $M = 2.5$ there still is a small elevation of the potential, but it remains negative. The potential enhancement disappears at lower M. In panel b), further downstream, such an enhancement in potential is not present for all cases except for $M = 4$ where a small bump is visible. For panel c), the wake is relatively symmetric for all cases, with only slight asymmetries visible. At about 20 Debye lengths, in Panel d), we see that some asymmetries in the potential depletion start to develop, especially for $M = 4$. In panel e) there is an asymmetry of the wake for $M = 4$. Lastly, for panel f), the wake for $M = 0.5$,1, and 2.5 are almost gone while, for $M = 4$, we can see a region in the wake where the potential has a relative enhancement. However, at such large distances, the potential variations are rather small, as also reflected in the scale of the vertical axis.

IV. DISCUSSION

A conductive body in the ionosphere will collect and emit currents (e.g., plasma, photoemission, secondary emission currents) and will attain a potential relative to the plasma. This floating potential will act in such a way so that all currents will balance and the net current to the surface vanishes[1,2]. Sounding rockets in the ionosphere usually attain a negative floating potential, since the relative contribution of the photoemission and secondary electron emission currents are small[21], and thus we have omitted them in our analysis. The main currents in the ionosphere driving the floating potential are then the ion and electron collection currents. In the polar ionosphere there is often a significant particle precipitation, which might affect the charging and the wake formation, but we do not consider it in the present study.

From FIG. 2 it is evident that the booms will have a significant effect on the ion density distribution around the rocket, and in turn, the plasma density as a whole. In this figure we have also restricted to a max of $M = 4$ since higher flow velocities are unrealistic for sounding rockets. For low M, i.e., panel a) and b), the main effect around the booms is focusing of ions near each tip, where the electric field is strongest, and as it can be infered from FIG. 8 this has a negligible effect on the wake. In FIG. 6 panel a) and b) the focusing

is similar between the two cases, but it is slightly weaker around Boom 2. The ion focusing depends on the strength of the electric field in the vicinity of the surface, and as one can see in FIG. 3 the potential differences between the plasma and booms at the edges are similar for $M = 0.5$ and 1, implying similar ion acceleration for the two cases. However, in FIG. 2 panel c) and d), the ion focusing to Boom 2 is smaller. The focusing around the tips of the booms is hence an edge effect, where one can expect the strongest electric fields and ion acceleration, which is further enhanced by the potential difference due to the convective electric field.

When M increases, the asymmetry in ion focusing around Boom 1 and Boom 2 develops. Furthermore, the focusing for $M = 2.5$ and $M = 4$ have lower peaks and are extending further than for smaller M, as shown in FIG. 6 panel a). This asymmetry and difference in focusing are due to a large potential gradient, as it is shown in FIG. 3, creating a significant difference in the potential difference at the edges of the booms. Away from the edge of Boom 1 (panel c) of FIG. 6), there are no significant focusing effects. As stated above, this is because the focusing is mainly the edge effect due to the booms. However, for the focusing to occur, there should be a sufficient potential difference, as can be infered by comparing cases with low M. For Boom 2, instead of focusing, a static wake characterized by ion depletion due to absorption on the rocket surface is formed (see again FIG. 6). This geometric wake gets affected at higher M by ion focusing at boom edges, which is a dynamic wake effect.

Since the booms are connected electrically to the main body, they will have an effect on the charging of the whole rocket. The ion and electron currents are different for each of the booms, as it can be seen in FIG 4. The ion currents to the two booms are very similar for all considered flow velocities. At low M, the currents are significantly different from the cold ion ram current given by Eg. (4). This can be attributed to thermal motion of the ions. Thermal ion motion is incorporated in Hoegy and Warthon's model[20], which indeed gives a better agreement with simulations. This is a similar result as from the study of McMahon, Xu, and Laframboise[22]. Small differences between the current to the booms might be attributed to different potential differences between the plasma and booms for each section of the booms due to potential gradient, as well as edge effects.

The electron currents to the booms are very different between the booms as compared to the ion currents, and this difference is increasing with M (see again FIG. 4). Since

electrons generally adjust to the potential much more efficient than ions, the difference between electron currents to the two booms can again be explained by the potential gradient leading to different potential differences between the booms and plasma. The potential drop for Boom 2 is lower than for Boom 1 (see again FIG. 3), which is also reflected in the currents. With Eq. (3) we derive an analytical expression of the total electron currents to the booms taking in account the different potential drops between the plasma and the surface of the boom for each section of the boom. Our result from Eq. (3) is in good agreement with the simulation results, but with a slight offset. This offset can be attributed to that Eq. (3) is derived without considering the edge of the booms. In general Eq. (3) can be used for any cylinder in a plasma that is aligned with the electric field when its potential is lower than the plasma potential and the electrons are Boltzmann distributed.

For the main body, the electron and ion currents differ significantly from Eqs. (4) and (5) at low flow speeds. We attribute this to the currents to the top and bottom of the cylinder, that is, Eqs. (4) and (5) are approximations using infinitely long cylinders with no edges as their geometry. For a cylinder with no booms the electron and ion currents will cancel each other out so that the cylinder draws no net current from the plasma, however we see that for high M the electron and ion current becomes significantly different. The ion current is still dominated by the ram current, but the electron current, which is much more sensitive to the potential of the object, is reflecting the very high increase in the electron currents Boom 2 is collecting at high M. That is, the main body's electron current is adjusting in order to maintain zero net current.

With subsonic plasma flow speeds there will be a significant ion current contribution from all sides of the rocket, but as the flow speed increases, less and less ions will be collected on the surface of the rocket facing downstream due to the development of a wake. In other words, the collection cross-section changes with increasing M. As can be seen in the right panel of FIG. 5 floating potential starts by becoming more negative. At around $M = 1.5$ the potential starts to be less negative. This is due to that the ion ram current becomes more significant as compared to the electron thermal current. The potential starts to increase at a lower rate with higher M, since Boom 2 collects an increased electron current.

It is evident that assumptions have been made regarding some of the plasma parameters in this study. For example the ion mass is much lower than the oxygen that is one of the main ion species of the ionosphere, which creates a much stronger convective electric fields

than those typically seen in the ionosphere[8,23]. However, note that for collection and ion focusing, one of the important factors is the potential difference between the plasma and the surface of the collector. Since the rocket model in our simulation has very short booms, the potential difference is still in a realistic regime[24]. One factor that is not represented well in this simulation is the force on the ions exerted by the electric potential of the body, which should in fact be much stronger than in reality. This might have an effect on the ion focusing and the asymmetry of the wake structures behind the rocket.

Understanding local plasma disturbances and charging of spacecrafts such as sounding rockets is important in order to estimate validity of measurements done by instruments on-board[24]. As shown in our study, measurements by rockets with instruments mounted on booms can experience difficulties due to local plasma disturbances. Thus, one needs to place instruments on booms in such a way as to minimize the risk of contaminating the data. Otherwise the data may not correspond to undisturbed plasma conditions. Due to the complex nature of the object-plasma interaction there it is not trivial to provide a generic model for any kind of additional structural elements to a sounding rocket and their impact on the measurements. This study provides insight on how booms will affect rocket-plasma interactions. Not only is there a strong asymmetry in the current collection from the booms, which can affect circuitry and the overall floating potential, but there is also a possibility of ion-focusing. The ion-focusing can extend far downstream, and may impact the measurements. As shown by this study, instruments further from the tips of the booms might be less effected. The results can also be applied to explain artifacts in data from sounding rocket experiments or similar spacecrafts.

V. CONCLUSION

With Particle-in-Cell simulations and analytical models, we have studied a cylindrically shaped rocked with booms in flowing ionospheric plasmas. It has been revealed that booms can have a significant effect on both the charging of the payload and disturbances of plasma in its vicinity. The electron and the ion currents to the booms are well approximated by analytical models, while for the main body there is a significant contributions from the top and the bottom of the rocket. Due to the potential gradient in flowing magnetized plasma, the booms collect different ion and electron currents, which are then compensated by the

currents to the main body. The difference between the ion and the electron currents increases with increasing flow velocity.

Edge effects on the booms lead to ion-focusing. For small Mach numbers it is contained within a small distance behind the booms. With increasing flow velocity the focusing is present at a significant distance downstream of the booms, which can be reflected in perturbations in the profile of the wake. Since most of the aspects of this study correspond to a reasonable degree with realistic sounding rocket experiment plasma conditions, the results can assist in a proper placement of instruments on such booms.

VI. ACKNOWLEDGMENETS

This work is the result of the Japan-Norway Partnership on Space Science Simulations, funded by the Norwegian Center for International Cooperation in Education SiU, grants UTF-2014/10043 and UTF-2016-long-term/10054, and it is a part of the 4DSpace Strategic Research Initiative at the University of Oslo. This study is supported in part by the Research Council of Norway grant no. 240000. The authors would also like to thank the participants of the Oslo-Kobe Workshop 2017 for their helpful contributions and advancements on subjects similar to the one presented in this study.

REFERENCES

[1]E. C. Whipple, Reports on Progress in Physics **44**, 1197 (1981).

[2]H. B. Garrett, Reviews of Geophysics **19**, 577 (1981).

[3]H. M. Mott-Smith and I. Langmuir, Physical Review **28**, 727 (1926).

[4]L. Schott (1971) p. 515.

[5]J. Moen, K. Oksavik, T. Abe, M. Lester, Y. Saito, T. A. Bekkeng, and K. S. Jacobsen, Geophysical Research Letters **39**, L07104 (2012).

[6]K. R. Svenes, J. Trim, B. N. Maehlum, M. Friedrich, K. M. Torkar, G. Holmgren, and W. F. Denig, Planetary and Space Science **38**, 653 (1990).

[7]D. A. Lorentzen, J. Moen, K. Oksavik, F. Sigernes, Y. Saito, and M. G. Johnsen, Journal of Geophysical Research: Space Physics **115**, A12323 (2010).

[8]A. Spicher, A. A. Ilyasov, W. J. Miloch, A. A. Chernyshov, L. B. N. Clausen, J. I. Moen, T. Abe, and Y. Saito, Journal of Geophysical Research: Space Physics **121**, 2016JA022999 (2016).

[9]Y. Miyake and H. Usui, Physics of Plasmas **16**, 062904 (2009).

[10]A. I. Eriksson, I. a. D. Engelhardt, M. Andr, R. Bostrm, N. J. T. Edberg, F. L. Johansson, E. Odelstad, E. Vigren, J.-E. Wahlund, P. Henri, J.-P. Lebreton, W. J. Miloch, J. J. P. Paulsson, C. S. Wedlund, L. Yang, T. Karlsson, R. Jarvinen, T. Broiles, K. Mandt, C. M. Carr, M. Galand, H. Nilsson, and C. Norberg, Astronomy & Astrophysics **605**, A15 (2017).

[11]Y. L. Al'pert, A. V. Gurevich, and L. P. Pitaevski, Soviet Physics Uspekhi **6**, 13 (1963).

[12]J. Wang and D. E. Hastings, Physics of Fluids B: Plasma Physics **4**, 1615 (1992).

[13]A. V. Gurevich, L. V. Pariskaya, and L. P. Pitaevski, Soviet Journal of Experimental and Theoretical Physics **36**, 274 (1973).

[14]V. C. Liu, Progress in Aerospace Sciences **16**, 273 (1975).

[15]U. Samir, M. First, E. J. Maier, and B. Troy, Journal of Atmospheric and Terrestrial Physics **37**, 577 (1975).

[16]E. Engwall, A. I. Eriksson, and J. Forest, Physics of Plasmas **13**, 062904 (2006).

[17]J. E. R.W Hockney, *Computer simulation using particles*, special student ed ed. (A. Hilger, 1988).

[18]W. J. Miloch and D. Block, Physics of Plasmas **19**, 123703 (2012).

[19]J. G. Laframboise and L. W. Parker, The Physics of Fluids **16**, 629 (1973).

[20]W. R. Hoegy and L. E. Wharton, Journal of Applied Physics **44**, 5365 (1973).

[21]R. J. L. Grard, Journal of Geophysical Research **78**, 2885 (1973).

[22]J. C. McMahon, G. Z. Xu, and J. G. Laframboise, Physics of Plasmas **12**, 062109 (2005).

[23]F. S. Mozer and P. Bruston, Journal of Geophysical Research **72**, 1109 (1967).

[24]J. J. P. Paulsson, A. Spicher, L. B. N. Clausen, J. I. Moen, and W. J. Miloch, Journal of Geophysical Research: Space Physics - Under revision (2018).

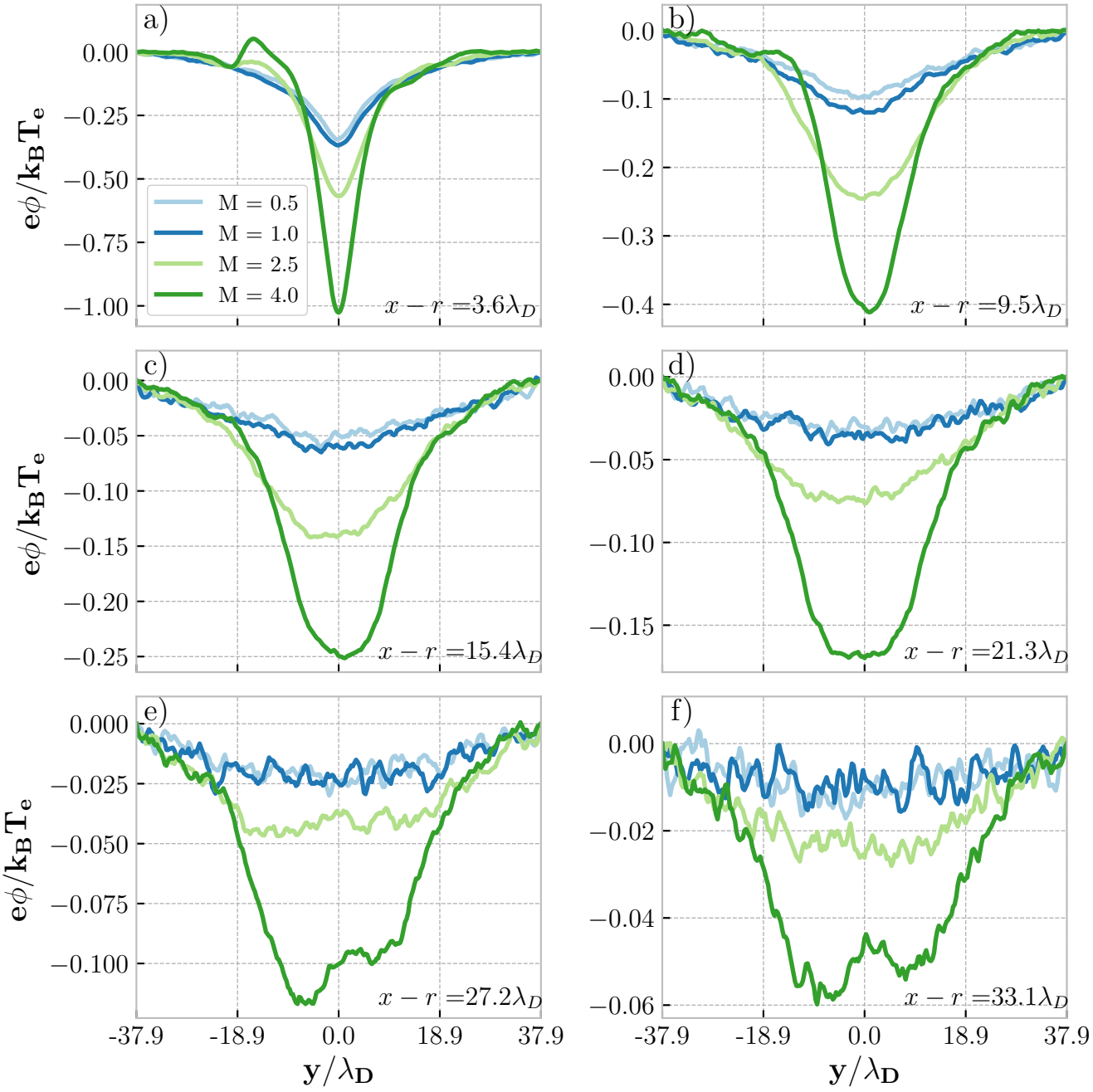

FIG. 8. The scaled potential profile behind the rocket taken along the y-axis, $z = 0$ and different distances from the rocket surface for different Mach numbers. Note that the scale of the vertical axis is different in each of the panels.